scientific reports

Check for updates

OPEN

# Network pharmacology to unveil the mechanism of Astragali Radix in the treatment of lupus nephritis via PI3K/AKT/mTOR pathway

Kuijun Zhan[1,4], Shuo Chen[3,4], Lina Ji[2,4], Liping Xu[2], Yan Zhang[2], Qi Zhang[2], Qiaoding Dai[2]✉ & Shan Wu[2]✉

**We used network pharmacology, molecular docking, and in vitro experiments to explore the mechanisms of Astragali Radix in the treatment of lupus nephritis. We screened compounds and targets of Astragali Radix, as well as related genes of lupus nephritis from databases. We identified 211 common genes and 44 compounds between the herb and the disease, and constructed global, narrowed, hierarchical Compound-Target Interaction networks to illustrate the possible mechanism. We found that the PI3K/AKT/mTOR pathway is a core target gene set identified through enrichment analysis, PPI analysis and MCODE analysis. In vitro experiments showed that freeze-dried Astragali powder inhibits activation of PI3K, AKT1 and mTOR in TGF-β1 stimulated HK-2 cells. Molecular docking demonstrated that (R)-isomucronulatol, 3,9,10-trimethoxypterocarpan and astrapterocarpan exhibited promising binding affinity to PI3K, AKT, and mTOR proteins.**

Lupus Nephritis (LN) is a severe complication of Systemic Lupus Erythematosus (SLE), significantly increasing the SLE-associated mortality and organ damage. It also diminishes the quality of life for patients[1]. Despite advancements in immunomodulatory therapies and supportive care, 5–30% of LN patients progress to end-stage kidney disease within 10 years of diagnosis[2,3]. Currently, belimumab and voclosporin have been approved for the management of LN, showing promise in improving patient outcomes[3]. Additionally, supplementary and complementary treatments are employed to enhance treatment efficacy and reduce toxicity, thereby controlling the disease progression[4].

Astragali Radix (AR), known as HuangQi in Chinese, is officially defined as the root of *Astragalus membranaceus(Fisch.) Bge.* or *A. membranaceus(Fisch.) Bge. var. mongholicus (Bge.) P. K. Hsiao*, in Pharmacopoeia of the People's Republic of China(2020 Edition)[5]. In Esat Asia, AR is frequently used for various kidney diseases, including Lupus Nephritis. High dose Astragali injection was co-administered with cyclophosphamide to enhance treatment efficacy in LN by reducing infections and proteinuria, and enhancing immune function[6]. The AR-centered TCM formulation, integrated with Western medicine, enhances treatment efficacy for LN by improving immune function and renal function while reducing medication-related side effects[7].

AR shows potential in treating kidney diseases by regulating inflammation, oxidative stress, fibrosis, endoplasmic reticulum stress, apoptosis, ferroptosis, and regulating autophagy[8]. Within the framework of Traditional Chinese Medicine, AR is thought to replenish 'kidney essence', a concept that refers to the fundamental substances vital for life, which is believed to be depleted in conditions presenting with proteinuria. Additionally, AR is considered to help restore fluid balance, thus reducing edema. However, the pharmacological mechanism of AR for LN remains uncertain.

Network medicine, grounded in network science and systems biology, serves as a pioneering approach to identify disease-specific modules and pathways. It also endeavors to investigate the molecular relationships among various pathological phenotypes[9]. Network pharmacology, as a specialized application of network medicine, has established a comprehensive workflow that is extensively utilized in the study of herbs[10]. To our knowledge, no prior network pharmacology analysis has been conducted to elucidate the therapeutic mechanism of AR in LN treatment. Therefore, we explored this mechanism through network pharmacology, in vitro experiments, and molecular docking (Fig. 1).

[1]The Second School of Clinical Medicine, Zhejiang Chinese Medical University, Hangzhou, China. [2]The First Affiliated Hospital of Zhejiang Chinese Medical University (Zhejiang Provincial Hospital of Chinese Medicine), Hangzhou, China. [3]The First School of Clinical Medicine, Zhejiang Chinese Medical University, Hangzhou, China. [4]These authors contributed equally: Kuijun Zhan and Shuo Chen. ✉email: 20043007@zcmu.edu.cn; zjtcm_doctorwu@163.com

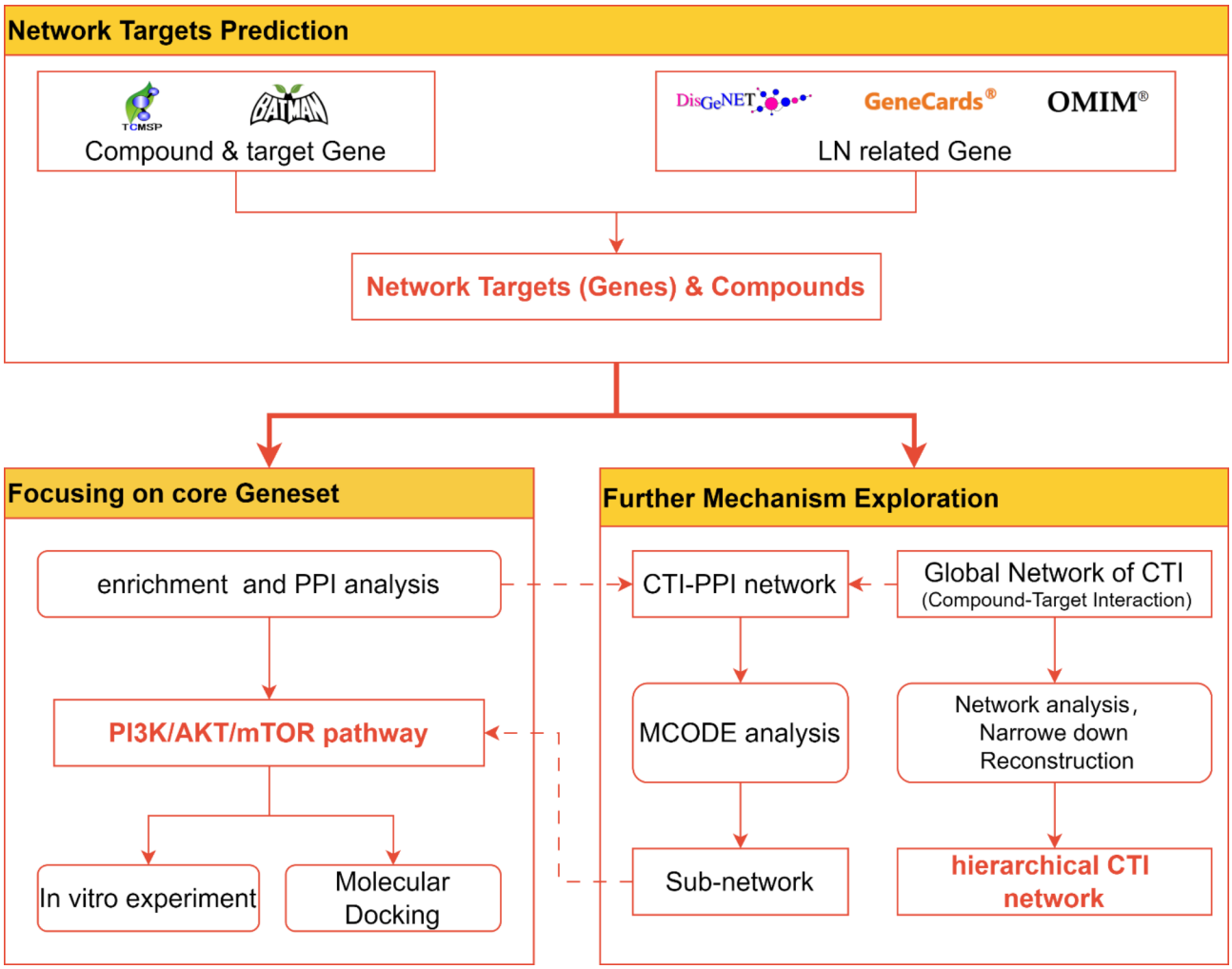


**Fig. 1**. Study workflow.

In TCM network pharmacology, the potential masking effect of homogeneous compounds can lead to biased research outcomes[11]. We mitigated this by removing these compounds to reduce their impact on network analysis. Additionally, recognizing the underappreciated role of low-degree nodes, we extracted them for potential significance. While not exhaustively analyzed, this approach aids in identifying key network players. The study was registered on OSF (https://doi.org/10.17605/OSF.IO/563ZP).

## Results

### Compounds and targets

We sourced compounds and their targets from TCMSP and BATMAN-TCM databases. Notably, although AR was absent in TCMSP[12], *Hedysarum multijugum Maxim (HMM)*, known as a substitute for AR, was listed and mapped to HuangQi. We merged HMM data with AR for our analysis, as most HMM compounds were also present in AR (Table 1). Ultimately, We identified 19 compounds and 1,139 targets from TCMSP, and 35 compounds and 962 targets from BATMAN-TCM[13].

The subsequent merge resulted in 44 unique compounds and 902 unique targets. Based on the classification system of natural medicines, we categorized these compounds into six types: alkaloids, flavonoids, steroids, terpenoids, stilbenoids, and others (Supplementary Table S1). Additionally, by combining data from GeneCards (1,332 genes)[19], OMIM (72 genes)[20], and DisGeNET (503 genes)[21], we identified 1,536 unique genes related to LN. Finally, we identified 211 genes that overlapped between AR and LN, which were considered potential targets.

### Target network of Astragali Radix ameliorating lupus nephritis

We constructed a global compound-target interaction (CTI) network to delineate the binary associations between compounds and targets. This global CTI network is segmented into several clusters. Cluster 4 is centered on DNMT1 and CXCR4, and the remaining clusters were compound-centric(Fig. 2A). Flavonoids predominantly formed the largest cluster (Cluster 1), while terpenoids and steroids are segregated into three clusters. Essential biomolecules such as guanosine and sucrose are primarily found in Cluster 5. Notably, 19

| | Reference |
|---|---|
| Compoud of HMM in AR | |
| *(2 S,3R,4 S,5 S,6R)-2-[[(3R)-3-[3,4-dimethoxy-2-[(2 S,3R,4 S,5 S,6R)-3,4,5-trihydroxy-6-(hydroxymethyl)oxan-2-yl]oxyphenyl]-3,4-dihydro-2 H-chromen-7-yl]oxy]-6-(hydroxymethyl)oxane-3,4,5-triol* | 14 |
| *(2 S,3R,4 S,5 S,6R)-2-[5-[(3R)-7-hydroxy-3,4-dihydro-2 H-chromen-3-yl]-2,3-dimethoxy-4-[(2R,3R,4 S,5 S,6R)-3,4,5-trihydroxy-6-(hydroxymethyl)oxan-2-yl] oxyphenoxy]-6-(hydroxymethyl)oxane-3,4,5-triol* | 14 |
| *(3s,8s,9s,10r,13r,14s,17r)-10,13-Dimethyl-17-[(2r,5s)-5-propan-2-yloctan-2-yl]2,3,4,7,8,9,11,12,14,15,16,17-dodecahydro-1 h-cyclopenta[a]phenanthren-3-ol* | 15 |
| *(R)-2,3-Dimethoxy-6-(7-methoxychroman-3-yl)phenol* | 14 |
| *(R)-Isomucronulatol* | |
| *3,9,10-Trimethoxypterocarpan* | 16 |
| *9,10-dimethoxypterocarpan-3-O-beta-D-glucoside* | 17 |
| *Astrapterocarpan* | 18 |
| *Calycosin* | 8 |
| *Folic acid* | 8 |
| *Hederagenin* | 8 |
| Uncertain compounds | |
| *Betulinic* Acid | |
| *Bifendate* | |

**Table 1**. Combined compounds from hedysarum multijugum maxim.

compounds, detailed in Supplementary Table S2, have unique connections to specific targets, predominantly 3,9,10-trimethoxypterocarpan and L-canavanine. Furthermore, key LN-related genes, such as JAK1, SELE, and HIF1A, are regulated by a limited number of these compounds.

Then the network was refined to a narrowed CTI network, which consists of 33 compounds and 76 targets to emphasize the key interactions (Supplementary Table S3). This network formed 2 neighboring large cores and 3 small cores (Fig. 2B). Next, we reconstructed a hierarchical network based on compound classifications and gene functions (Fig. 2C), in which the flavonoid group (C3) affects all gene groups except T5 and exclusively regulates the T4 group (Supplementary Fig S4). We also established a functional modules CTI network based on KEGG pathway enrichment analysis results (Supplementary Fig S5). These networks collectively provide a comprehensive landscape of AR's role in LN treatment.

## Focusing on the PI3K/AKT/mTOR pathway

Through enrichment analysis, we identified 91 gene ontology (GO)[22] molecular function (MF) terms, 50 GO cellular component (CC) terms and 660 GO biological process (BP) terms. Additionally, we identified 181 Kyoto Encyclopedia of Genes and Genomes (KEGG)[23,24] pathway terms and 280 Reactome[25] pathway terms. The PI3K/AKT/mTOR pathway was prominent among the top GeneRatio terms, correlating with nearly half of the Reactome terms and the majority of the KEGG and GO terms (Fig. 3A). Furthermore, Protein-Protein Interaction (PPI) analysis revealed that the genes with the highest degrees of interaction include SRC, HSP90AA1, PIK3CA/B/D and AKT, mTOR, PTPN11, JAK1/2, etc. (Figs. 3B). These findings underscore the crucial role of the PI3K/AKT/mTOR pathway in the target network.

The PI3K/AKT/mTOR pathway genes also play an important role in sub-network. The MCODE (Molecular Complex Detection), a Cytoscape plugin, uses the Score value as an indicator to measure the importance of sub-networks. We extracted eight sub-networks from the combined CTI-PPI network using MCODE (Supplementary Fig. S6). Cluster1 and Cluster2 are refined networks derived from the highest-scoring sub-networks, featuring molecules from the PI3K/AKT/mTOR pathway. Cluster1 (score = 21.509) centers around the genes JAK2, AKT1, and the compound 3,9,10-trimethoxypterocarpan; Cluster2 (score = 4.875) centers around the genes MARK, PI3Ks, and the compounds 3,9,10-trimethoxypterocarpan, (R)-Isomucronulatol (Supplementary Fig. 2). Simplified module diagrams of these two clusters show the function of PIK3CB, PIK3CD and AKT1 within sub-network (Fig. 3C).

## Astragali Radix inhibits the PI3K/AKT1/mTOR pathway in HK-2 cells induced by TGF-β1

We assessed the influence of AR on the TGF-β1-induced activation of the PI3K/AKT1/mTOR pathway in HK-2 cells to validate the effects of AR on this pathway in LN. The TGF-β1-induced HK-2 cell could serves as an in vitro model of renal interstitial fibrosis[26]. Within our predefined concentration gradients, freeze-dried AR powder promoted HK-2 cell proliferation without determining the IC50. Given our preliminary focus on exploring AR's impact on the PI3K/AKT/mTOR pathway, we did not increase the concentrations beyond our initial range. Consequently, we selected 0.25, 0.5, and 1 mg/mL for subsequent experiments(Fig. 4A).

In TGF-β1 stimulated HK-2 cells, mRNA expression of AKT1 and MTOR was elevated, along with increased protein levels of PI3K-p85, mTOR, p-AKT1, and p-mTOR. However, AR powder reversed these increases, and the effect was correlated with the concentration of AR powder(Figs. 4B–D, 5A–F, Supplementary Fig. 7). These results suggest that AR could inhibit the PI3K/AKT1/mTOR pathway.

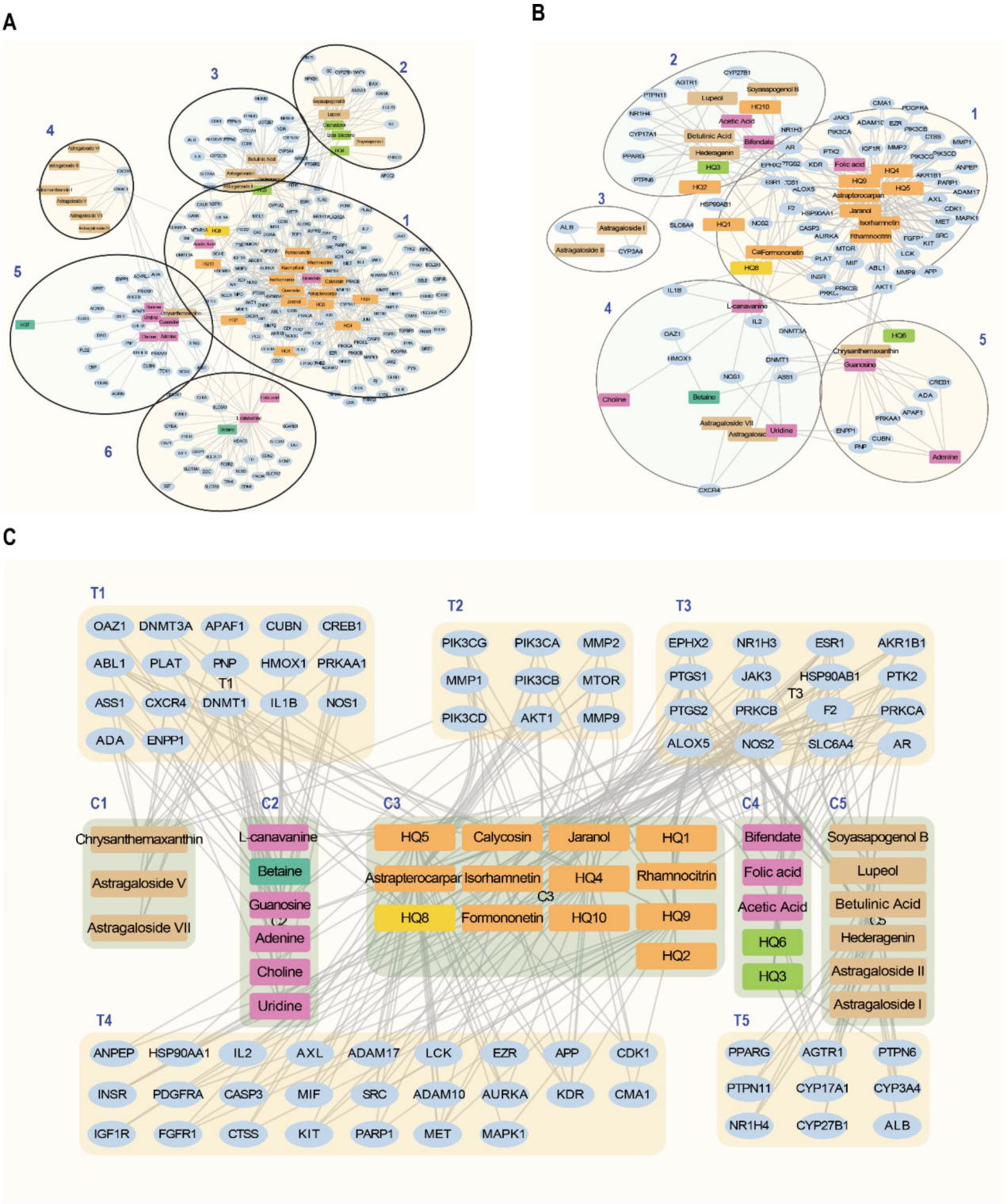


**Fig. 2**. Force-directed graph of the compound-target interactions. Gene nodes are gray, while compound nodes are colorful. (**A**) Global CTI network (*parameter: default*). (**B**) Narrowed CTI network (*parameters: Iterations = 120, Spring Length = 100, Force-Directed Edge Bundling = default*). (**C**) Hierarchical CTI network, organized based on compound classifications.

## Identification of potential Astragali Radix compounds regulating the PI3K/AKT/mTOR pathway

We identified compounds regulating the PI3K/AKT/mTOR pathway by their binding affinities to specific target proteins. After identifying compounds in the sub-network that target PIK3CA, PIK3CB, PIK3CD,

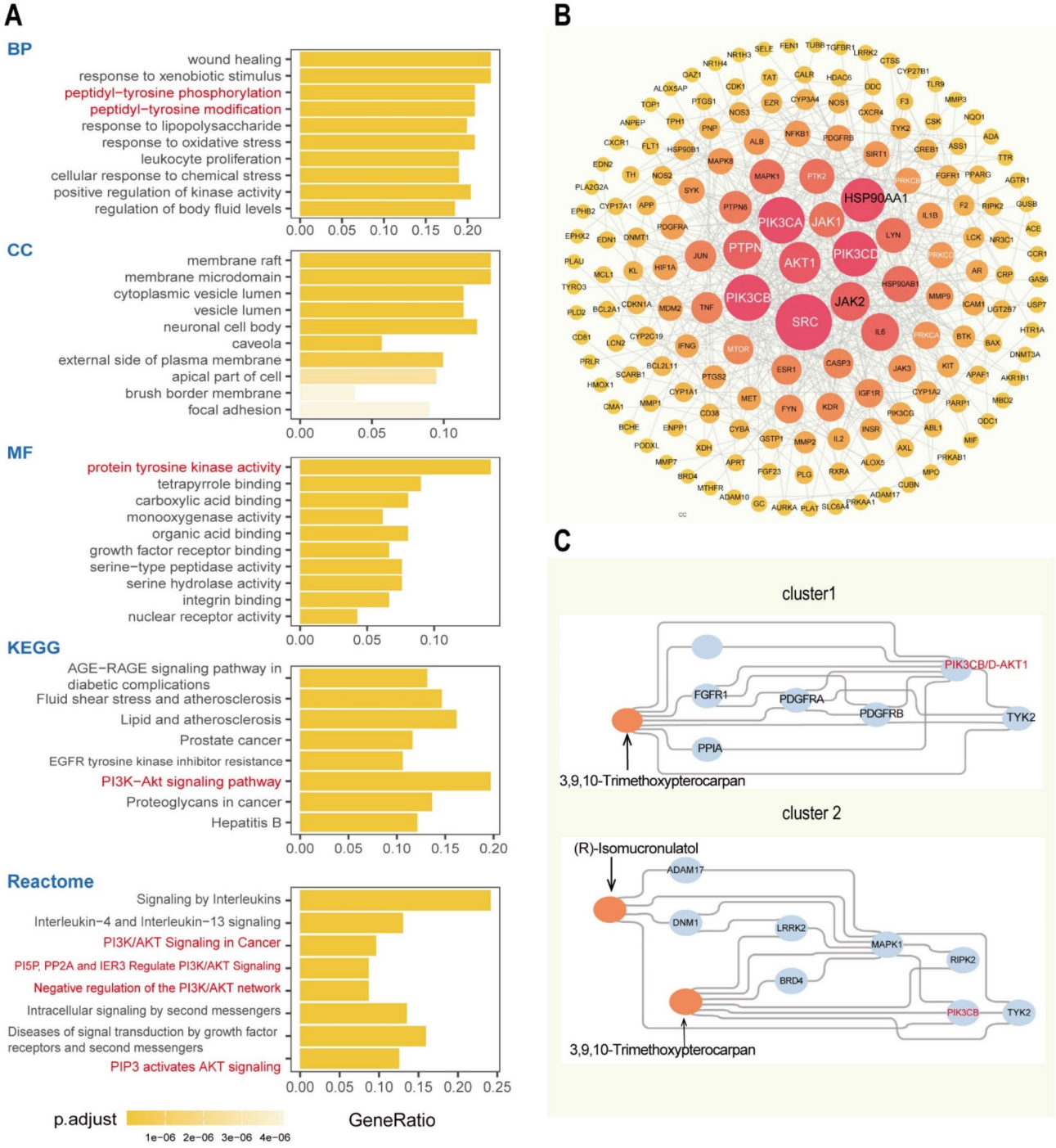


**Fig. 3**. Enrichment, PPI and sub-network analysis. (**A**) The top ten simplified enrichment terms for GO–BP, GO–CC, GO–MF, as well as the top eight terms for KEGG pathway and Reactome pathway enrichment. (**B**) PPI network of AR in the treatment of lupus nephritis. (**C**) The principal compounds in AR targeting the PI3K/AKT/mTOR pathway and their underlying mechanisms.

PIK3CG, AKT1, and mTOR, we excluded sitosterols, quercetin, kaempferol, and other nutritional compounds. Subsequently, (R)-isomucronulatol, 3,9,10-trimethoxypterocarpan, and astrapterocarpan were identified and subjected to molecular docking with the targets. Affinities ranged from −7.1 to -8.9, suggesting these compounds bind readily to their target proteins (Fig. 6). Notably, although 3,9,10-trimethoxypterocarpan and astrapterocarpan were not linked to AKT1 in our CTI network, they still demonstrated low binding energies. These results only suggest potential interactions, not a direct mechanism.

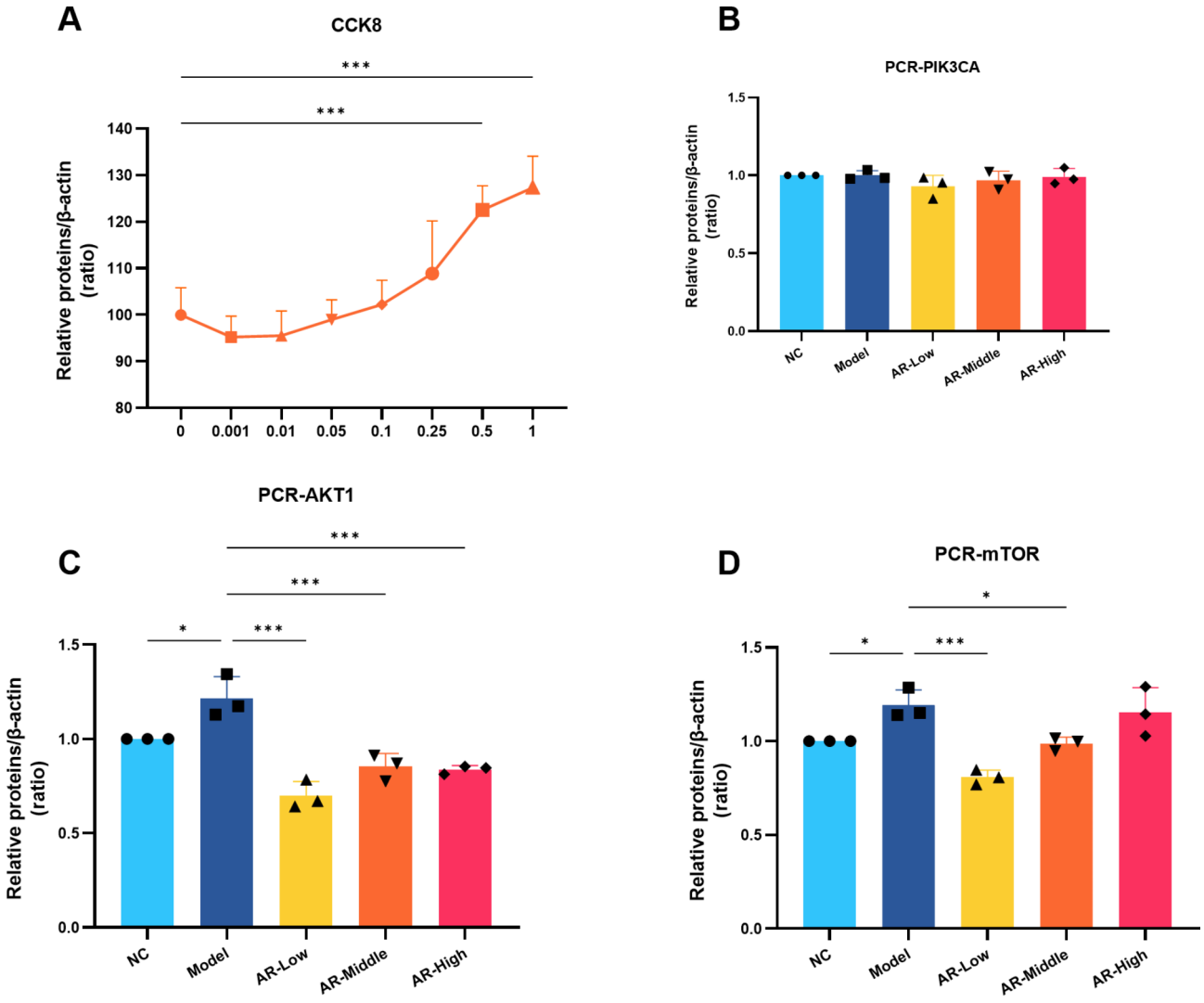


**Fig. 4**. The mRNA expression of PI3K/AKT/mTOR in HK-2 cells stimulated by TGF-β1. (**A**) Cell viability HK-2 cells treated with different concentrations of Astragali Radix. (**B**–**D**) The mRNA expression of PIK3CA, AKT1 and mTOR as determined by real-time PCR (*$p < 0.05$; **$p < 0.01$; ***$p < 0.001$). AR-low, AR-middle, and AR-high groups are treated with freeze-dried AR powder at concentrations of 0.25, 0.5, and 1 mg/mL, respectively.

## Discussion

Clinical trials and experimental research have confirmed that AR can ameliorate LN by enhancing metabolic activity and regulating immune responses, yet the underlying mechanisms are not fully understood. In this study, we explored the potential compounds and their targets using network pharmacology, a method widely used to investigate the therapeutic mechanisms of Traditional Chinese Medicine. Previous research has employed network pharmacology to investigate the mechanism of *Hedyotis Diffusae Herba*[27] and luteolin[28] in treating LN, demonstrating the feasibility of this method. To elucidate more specific mechanisms, we implemented two targeted strategies. Firstly, we removed homologous compounds, which are found across various herbs and correlate with numerous diseases. The widespread presence of these compounds may potentially obscure more specific bioactive compounds[11]. For example, quercetin targets 154 genes, whereas astragaloside impacts only 6 genes. This significant disparity in the number of genes could potentially underestimate the importance of astragaloside in the CTI networks. Secondly, we focused on low-degree nodes, which are connected to fewer nodes. While high-degree genes are crucial in the PPI network[9], compounds targeting low-degree target genes are equally important for their unique function in the CTI network. For instance, PLAU gene is primarily regulated by calycosin, and JAK1/JAK2/SELE are specifically modulated by 3,9,10-trimethoxypterocarpan; these compounds serve as bottlenecks in the network.

Enrichment analysis revealed the central role of PI3K/AKT/mTOR pathway in the therapeutic efficacy of AR against LN. This pathway, which is critical for regulating cell growth, proliferation and metabolism[29,30], is also implicated in the pathogenesis of SLE[31]. Activation of PI3K/AKT/mTOR pathway in LN murine[32], and mTORC1/2 in LN patients[33], implicates this pathway as a pathological feature of LN. This pathway could

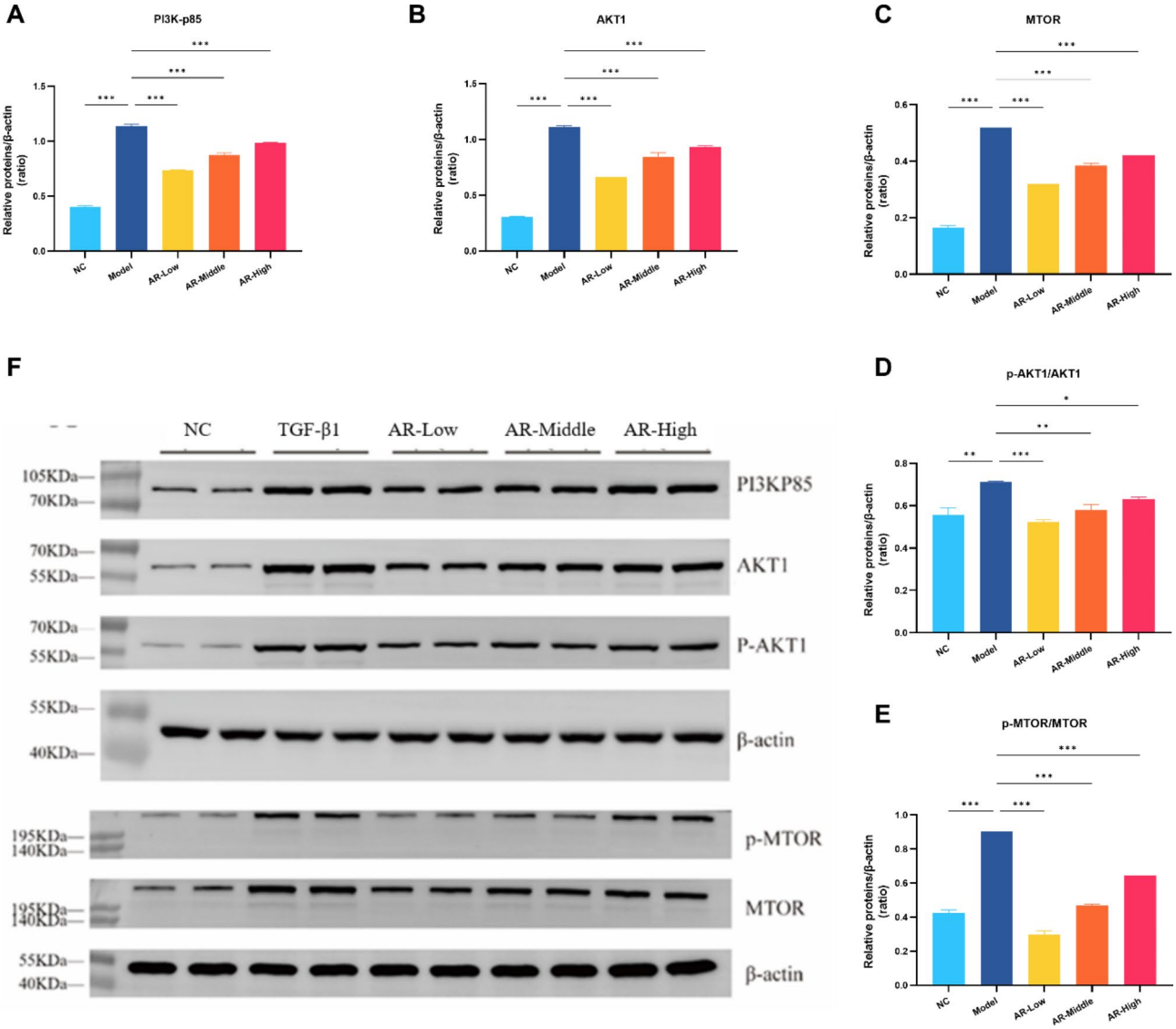


**Fig. 5**. Astragali Radix inhibited the PI3K/AKT/mTOR pathway in HK-2 cells stimulated by TGF-β1. The samples were derived from the same experiment and blots were processed in parallel. (**A**–**C**) Quantitative analysis of expression of PI3K p85, AKT1, mTOR. (**D**–**E**) Phosphorylation levels of AKT1 and MTOR. (**F**) The protein bands and original blots are presented in (Supplementary Figure S7).

mediates TWEAK, regulates HMGB1, NF-κB pathway and Fas pathway, thereby exacerbating the pathogenesis of LN[34,35]. Subsequent in vitro experiments have shown the activation of this pathway in TGF-β1 stimulated HK-2 cells, and AR was shown to suppress this activation. Previous studies have demonstrated that rapamycin can inhibit the progression of LN mice by downregulating the PI3K/AKT/mTOR pathway[32], and that trifluoperazine triggers apoptosis by downregulating AKT phosphorylation in LN mesangial cells[36]. Collectively, these findings underscore the significance of targeting the PI3K/AKT/mTOR pathway in LN treatment; it may represent a key mechanism through which AR exerts its effects on LN. Notably, the expression of mTOR and associated genes does not inversely correlate with AR concentrations, warranting further exploration to elucidate the underlying complex mechanisms. Moreover, our findings, validated only at the cellular level, may not fully predict in vivo outcomes, suggesting limitations in physiological relevance. In subsequent studies, we plan to construct animal models and employ high-throughput sequencing to identify more specific targets, subsequently validate them in vivo.

Network analysis suggests that (R)-isomucronulatol, 3,9,10-trimethoxypterocarpan and astrapterocarpan are potentially key compounds targeting the PI3K/AKT/mTOR pathway. Among these, astrapterocarpan has been shown to inhibit AKT phosphorylation in platelet-derived growth factor-BB-induced rat vascular smooth muscle cells (PDGF-BB-induced A10 cells)[18]. Besides, the network analysis indicates that AR affects not only the PI3K/AKT/mTOR pathway but also other pathways, such as TLR, NF-κB, JAK/STAT, TCR, BCR, TH17, and IL-17 pathways. In the context of LN, TLR, NF-κB, and JAK/STAT pathways play a pivotal role in innate immune responses by modulating interferons (IFNs), whereas the TCR, BCR, TH17, and IL-17 pathways significantly

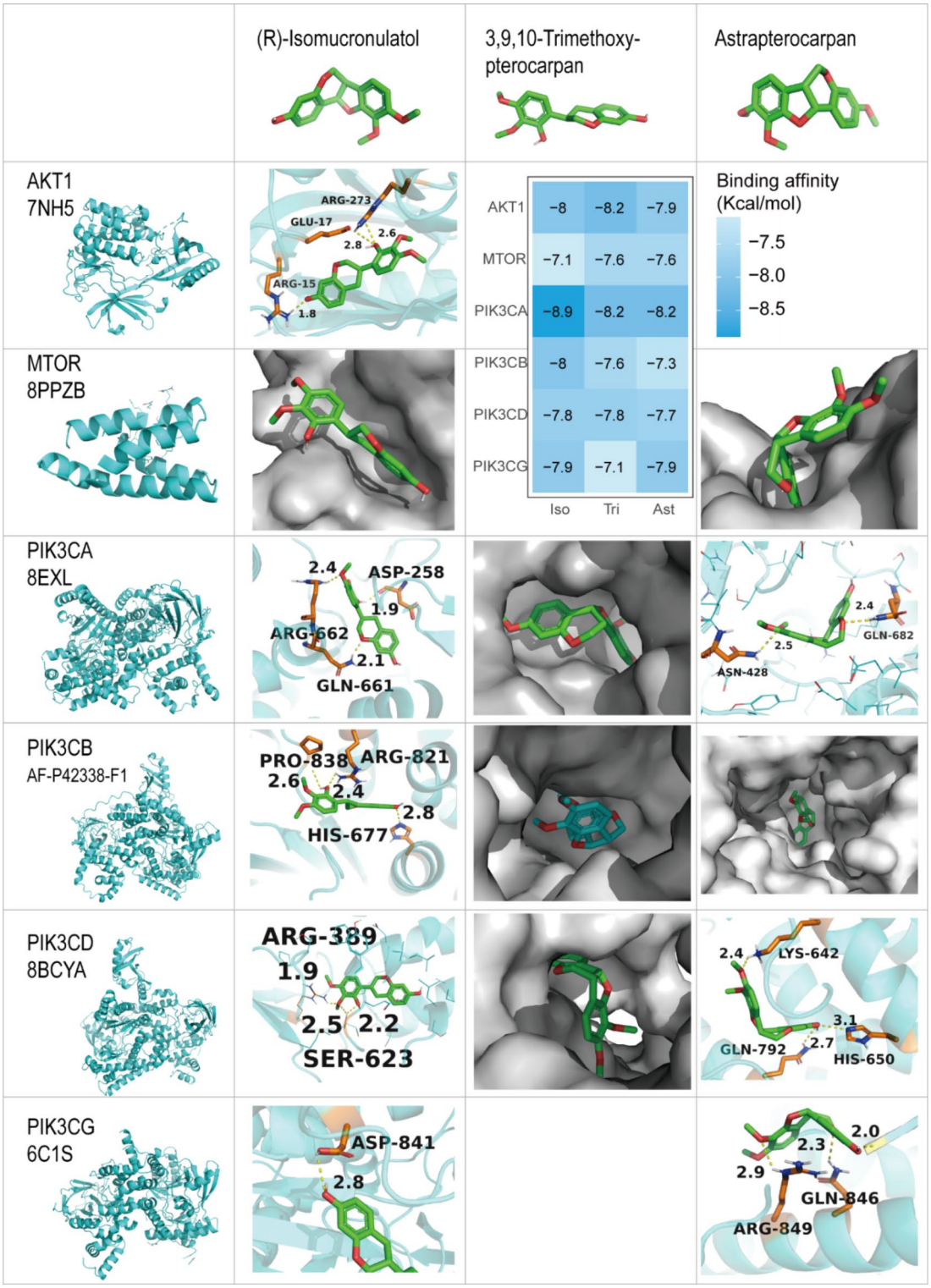


**Fig. 6**. Molecular docking. The heatmap figure represents the overall binding energy. In cartoon model, the dotted lines represent the hydrogen bond, and the text labels indicate the residue name. The surface model represents the absence of direct hydrogen bonds.

contribute to adaptive immune responses[37]. That indicates AR may provide therapeutic benefits in LN via multiple mechanisms.

However, our network analysis may have limitations and biases. Firstly, key bioactive compounds of AR, such as astramembrannin I, calycosin, astragalus polysaccharide, and astragalosides[8], exhibit unexpectedly lower degree in the CTI network despite their diverse functions. This phenomenon could be due to incomplete

compound and target data for AR. For example, the absence of astragalus polysaccharides in the compounds, and the under-representation of Astragaloside I targets (only 4 from the database versus 100 listed in PubChem[38]), could introduce a bias in degree. Incomplete data also mislead analysis on compound-target interactions. While the CTI network shows 3,9,10-trimethoxypterocarpan as the sole regulator of JAK1, research has indicated that Astragaloside IV could inhibit the JAK1/STAT1 pathway[39]. A comprehensive literature review, coupled with LC-MS/MS for compound identification and multi-omics for target identification, is likely to enhance the accuracy of the analysis. Secondly, these networks remain complex, potentially limiting their ability to succinctly profile the mechanisms. Constructing biofunctional target modules based on prior knowledge[40], or predicting gene modules with statistical and machine learning[41,42], may reveal deeper insights.

In conclusion, our comprehensive analysis elucidated potential compounds and mechanisms of Astragali Radix in treating Lupus Nephritis. The modulation of PI3K/AKT/mTOR pathway by (R)-isomucronulatol, 3,9,10-trimethoxypterocarpan and astrapterocarpan emerged as a key mechanism. These findings offer a rationale for AR's clinical advancement in LN treatment.

## Methods

### Identification of compounds and targets

TCMSP database and BATMAN-TCM database were queried using keywords "*Astragali Radix*" and "HuangQi" to identify relevant compounds and targets. From the TCMSP, compounds were selected based on a Drug-likeness (DL) $\geq 0.18$ and an oral bioavailability (OB) $\geq 30\%$, along with their corresponding targets. Similarly, compounds and targets that met a 10% cutoff were retrieved from BATMAN-TCM. To enhance robustness and minimize redundancy from prediction, we deliberately eschewed tools like Swiss-Target Prediction for target prediction of compounds. Compounds were unified using PubChem name, and targets were converted to gene names using UniProt KB data (release April 2023). Simultaneously, GeneCards, OMIM and DisGeNET were searched using the keyword "Lupus Nephritis" to identify relevant genes.

### Construction and refinement of compound-traget interaction network

We used Cytoscape 3.10.1[43] to construct various CTI networks. To refine a narrowed CTI network, we removed single-linked compounds and targets and excluded homogeneous compounds such as β-Sitosterol, γ-Sitosterol, Quercetin, Kaempferol, and Sucrose. Additionally, we also identified significant targets using PPI data from STRING (version 3.8) with a cutoff $> 0.9$[44]. Subsequently, the narrowed CTI network was restructured into a hierarchical form based on topological structure and prior knowledge. Furthermore, we selected SLE and LN-associated pathways from KEGG enrichment analysis to construct a functional module CTI network.

### Enrichment, PPI and sub-network analysis

To find out crucial genes, all targets were selected for enrichment analysis using the R package clusterprofiler and ReactomePA for GO, KEGG pathway, and Reactome pathway. P-values were adjusted using Benjamini-Hochberg methods. Redundancy in enriched GO terms was simplified using "Wang" methods. Terms with a p.adjust-value below 0.05 were retained. Additionally, PPI data were imported into Cytoscape for network analysis to identify hub genes by degree.

Based on the hypothesis that compounds modulate gene networks to treat diseases[45], we employed the MCODE to identify sub-network[46]. MCODE uses graph theoretic clustering algorithm to discover molecular complexes, which form sub-networks within the global network. After merging the CTI and PPI networks into a unified CTI-PPI network, we applied the MCODE algorithm to this integrated network.

### Freeze-dried Astragali powder preparation

AR was obtained from Zhejiang Chinese Medical University Medical Pieces. LTD (Hangzhou, China). AR was immersed in 400 mL of water for 30 min and then boiled for an additional 30 min; this process was repeated twice. The two water extracts were combined and concentrated to a final concentration of 1 g/mL using a rotary evaporator. The supernatant was then frozen at −20 °C for 2 h and subsequently freeze-dried for 72 h in a freeze-dryer to obtain the freeze-dried AR powder.

### Cell culture and model establishment

The HK-2 cell line was acquired from Fu Heng Biology (Shanghai, China). HK-2 cells were cultured in DMEM/F12 containing 10% fetal bovine serum (FBS) and 1% penicillin/streptomycin at 37℃, 5% CO2. In their logarithmic growth phase, HK-2 cells were seeded into a 6-well plate and allowed to adhere for 24 h. Cells were subsequently divided into five groups: control, model, AR low-dose, AR medium-dose, and AR high-dose groups. The control group received regular DMEM/F12, whereas the other groups were treated with TGF-β1 (10 ng/ml, MedChemExpress, USA). After 24 h, the AR groups were treated with AR powder. Cells were incubated at 37 ℃, 5% CO2 for 24 h.

### Cell viability assays

HK-2 cells were seeded in 96-well plates at a density of $5 \times 10^3$ cells/well. After adherence, the cells were treated with AR powder at concentrations of 0, 0.001, 0.01, 0.05, 0.1, 0.25, 0.5 and 1 mg/ml. After 24 h, the culture medium was aspirated, and Cell Counting Kit-8 (CCK-8) reagent (Beyotime, Shanghai, China) was added to the wells. Absorbance was measured using a microplate reader (PerkinElmer, Enspire, MA, USA).

### Real-time quantitative polymerase chain reaction

Total RNA was extracted from cells using RNAiso Plus (9108Q, Takara, Japan). The concentration of total RNA was measured by NanoDrop One (Thermo, USA). Reverse transcription of the RNA was carried out using the

| Gene | Forward sequence | Reverse sequence |
|---|---|---|
| Human PIK3CA | CCACGACCATCATCAGGTGAA | CCTCACGGAGGCATTCTAAAGT |
| Human MTOR | ATGCTTGGAACCGGACCTG | TCTTGACTCATCTCTCGGAGTT |
| Human AKT1 | CCTCCACGACATCGCACTG | TCACAAAGAGCCCTCCATTATCA |

**Table 2**. Primers used for RT-qPCR.

reverse transcription kit (AG11728, Accurate Biotechnology, China). SYBR Green qPCR Kit (AG11701, Accurate Biotechnology, China) was used to detect the expression of genes using Light Cycler 96 (Roche, Switzerland), and GAPDH was used as an endogenous control. The primer sequences are listed in (Table 2).

### Western blot

Total cellular proteins were extracted using RIPA buffer (Servicebio, Wuhan, China) and the concentration of each sample was determined using a BCA kit (Servicebio, Wuhan, China). Protein samples were separated using 10% SDS-PAGE gel and subsequently transferred onto 0.45 μm PVDF membranes. Membranes were blocked with 5% non-fat milk dissolved in TBST for 2 h, followed by cutting the membranes based on full-membrane blot and the theoretical molecular weights. After washing with TBST, Antibodies against AKT1 (GB111114, Servicebio), mTOR (GB111839, Servicebio), p-mTOR (GB114489, Servicebio), β-actin (GB15001, Servicebio), PI3K P85(ET1608-70, HUABIO, China), and p-AKT-S473 (ET1607-73, HUABIO) were added and incubated or 12 h at 4 ℃. After washing with TBST, the membranes were incubated with the corresponding horseradish peroxidase-conjugated secondary antibodies for 2 h at room temperature. Protein bands were visualized using an ECL kit (G2014-100ML, Servicebio) on the ChemiDoc system (BIO-RAD, CA, USA). β-actin was selected as the loading control, and the images were analyzed using ImageJ 1.53[47].

### Molecular docking

Compound structures were downloaded from PubChem and converted using Open Babel[48]. Protein 3D structures were obtained from the RCSB Protein Data Bank[49] or the AlphaFold Protein Structure Database[50], considering factors such as resolution, release time, and the composition of macromolecular chain. The required protein chain was extracted using PyMol-open-source (Schrödinger, LLC). AMdock was used for automatic preprocessing, molecular docking and visualization[51].

### Statistical analysis

All experimental data are presented as the mean ± SD. Data were analyzed using one-way ANOVA followed by Dunnett's multiple comparisons test with Prism 9 software (GraphPad Software). A $P$-value of $< 0.05$ was considered to indicate statistical significance.

## Data availability

The raw data used to obtain the network target, the overlapped 211 genes between AR and LN, the interactive CTI network graph, and detailed information on the MCODE sub-network diagram are available on figshare (https://doi.org/10.6084/m9.figshare.25827103).

Received: 17 May 2024; Accepted: 25 October 2024
Published online: 29 October 2024

## References

1. Mok, C. C., Teng, Y. K. O., Saxena, R. & Tanaka, Y. Treatment of lupus nephritis: consensus, evidence and perspectives. *Nat. Rev. Rheumatol.* **19**, 227–238 (2023).
2. Parikh, S. V., Almaani, S., Brodsky, S. & Rovin, B. H. Update on lupus nephritis: Core curriculum 2020. *Am. J. Kidney Dis.* **76**, 265–281 (2020).
3. Fanouriakis, A. et al. EULAR recommendations for the management of systemic lupus erythematosus: 2023 update. *ARD* **83**, 15–29 (2024).
4. Liu, L., Zhang, L. & Li, M. Application of herbal traditional Chinese medicine in the treatment of lupus nephritis. *Front. Pharmacol.* **13**, 981063 (2022).
5. Pharmacopoeia of the People's Republic of China (2020 Edition), Astragali Radix. (2024).
6. Li & Su Jianchun Mao, & Junhua Gu. Effect of intravenous drip infusion of cyclophosphamide with high-dose Astragalus injection in treating lupus nephritis. *Chin. J. Integr. Med.* 272–275 (2007).
7. Benli Chen. *The clinical study on the combined treatment of lupus nephritis Based on Chinese medicine mainly consisting of astragalus in two step sequential with western medication* (Guangxi University of Chinese Medicine, 2018).
8. Shi, Y., Shi, X., Zhao, M., Ma, S. & Zhang, Y. Pharmacological potential of Astragali Radix for the treatment of kidney diseases. *Phytomedicine* **123**, 155196 (2024).
9. Barabási, A. L., Gulbahce, N. & Loscalzo, J. Network medicine: A network-based approach to human disease. *Nat. Rev. Genet.* **12**, 56–68 (2011).
10. Wang, X., Wang, Z. Y., Zheng, J. H. & Li, S. TCM network pharmacology: A new trend towards combining computational, experimental and clinical approaches. *Chin. J. Nat. Med.* **19**, 1–11 (2021).
11. Zeng, P. Zhou,Hang. Homogenization of key components screening of 'different diseases and different prescriptions' in network pharmacology. *Chin. J. Exp. Traditional Med. Formulae* **28**, 177–191 (2022).
12. Ru, J. et al. TCMSP: a database of systems pharmacology for drug discovery from herbal medicines. *J. Cheminform.* **6**, 13 (2014).
13. Kong, X. et al. BATMAN-TCM 2.0: an enhanced integrative database for known and predicted interactions between traditional Chinese medicine ingredients and target proteins. *Nucleic Acids Res.* **52**, D1110–D1120 (2024).

14. Subarnas, A., Oshima, Y. & Hikino, H. Isoflavans and a pterocarpan from astragalus mongholicus. *Phytochemistry* **30**, 2777–2780 (1991).
15. Zhang, Y. et al. Efficacy and safety of the Chinese herbal compound TJAOA101 in treating diminished ovarian reserve: A protocol for multicenter, prospective, and pre-post study. *Curr. Med. Sci.* **43**, 284–296 (2023).
16. Song, J. Z., Yiu, H. H. W., Qiao, C. F., Han, Q. B. & Xu, H. X. Chemical comparison and classification of Radix Astragali by determination of isoflavonoids and astragalosides. *J. Pharm. Biomed. Anal.* **47**, 399–406 (2008).
17. Yu, D., Duan, Y., Bao, Y., Wei, C. & An, L. Isoflavonoids from Astragalus mongholicus protect PC12 cells from toxicity induced by L-glutamate. *J. Ethnopharmacol.* **98**, 89–94 (2005).
18. Ohkawara, S., Okuma, Y., Uehara, T., Yamagishi, T. & Nomura, Y. Astrapterocarpan isolated from astragalus membranaceus inhibits proliferation of vascular smooth muscle cells. *Eur. J. Pharmacol.* **525**, 41–47 (2005).
19. Stelzer, G. et al. The geneCards suite: From gene data mining to disease genome sequence analyses. *CP Bioinf.* **54**, (2016).
20. Amberger, J. S., Bocchini, C. A., Scott, A. F. & Hamosh, A. OMIM.org: leveraging knowledge across phenotype-gene relationships. *Nucleic Acids Res.* **47**, D1038–D1043 (2019).
21. Piñero, J. et al. The DisGeNET knowledge platform for disease genomics: 2019 update. *Nucleic Acids Res.* **48**, D845–D855 (2020).
22. Ashburner, M. et al. Gene ontology: tool for the unification of biology. *Nat. Genet.* **25**, 25–29 (2000).
23. Kanehisa, M. & Goto, S. KEGG: kyoto encyclopedia of genes and genomes. *Nucleic Acids Res.* **28**, 27–30 (2000).
24. Kanehisa, M., Sato, Y., Kawashima, M., Furumichi, M. & Tanabe, M. KEGG as a reference resource for gene and protein annotation. *Nucleic Acids Res.* **44**, D457–462 (2016).
25. Milacic, M. et al. The reactome pathway knowledgebase 2024. *Nucleic Acids Res.* **52**, D672–D678 (2024).
26. Wu, S. et al. Jieduquyuzishen prescription attenuates renal fibrosis in MRL/lpr mice via inhibiting EMT and TGF-β1/Smad2/3 pathway. *Evid. Based Complement. Alternat. Med.* 4987323 (2022).
27. Yang, J. & Li, S. Molecular mechanism of hedyotis diffusae herba in the treatment of lupus nephritis based on network pharmacology. *Front. Pharmacol.* **14**, 1118804 (2023).
28. Ding, T. et al. Luteolin attenuates lupus nephritis by regulating macrophage oxidative stress via HIF-1α pathway. *Eur. J. Pharmacol.* **953**, 175823 (2023).
29. Bilanges, B., Posor, Y. & Vanhaesebroeck, B. PI3K isoforms in cell signalling and vesicle trafficking. *Nat. Rev. Mol. Cell. Biol.* **20**, 515–534 (2019).
30. Yu, J. S. L. & Cui, W. Proliferation, survival and metabolism: the role of PI3K/AKT/mTOR signalling in pluripotency and cell fate determination. *Development* **143**, 3050–3060 (2016).
31. Beşliu, A. N. et al. PI3K/Akt signaling in peripheral T lymphocytes from systemic lupus erythematosus patients. *Roum Arch. Microbiol. Immunol.* **68**, 69–79 (2009).
32. Stylianou, K. et al. The PI3K/Akt/mTOR pathway is activated in murine lupus nephritis and downregulated by rapamycin. *Nephrol. Dial. Transplant.* **26**, 498–508 (2011).
33. Mao, Z. et al. Renal mTORC1 activation is associated with disease activity and prognosis in lupus nephritis. *Rheumatology* **61**, 3830–3840 (2022).
34. Nowling, T. K. Mesangial cells in lupus nephritis. *Curr. Rheumatol. Rep.* **23**, 1–10 (2021).
35. Cristofano, A. D. et al. Impaired fas response and autoimmunity in Pten+/– mice. *Science* **285**, 2122–2125 (1999).
36. Wang, B., Luo, Y., Zhou, X. & Li, R. Trifluoperazine induces apoptosis through the upregulation of Bax/Bcl–2 and downregulated phosphorylation of AKT in mesangial cells and improves renal function in lupus nephritis mice. *Int. J. Mol. Med.* **41**, 3278–3286 (2018).
37. Mohan, C., Zhang, T. & Putterman, C. Pathogenic cellular and molecular mediators in lupus nephritis. *Nat. Rev. Nephrol.* **19**, 491–508 (2023).
38. Sayers, E. W. et al. Database resources of the national center for biotechnology information. *Nucleic Acids Res.* **50**, D20–D26 (2022).
39. Zhou, X. et al. Astragaloside IV from astragalus membranaceus ameliorates renal interstitial fibrosis by inhibiting inflammation via TLR4/NF-κB in vivo and in vitro. *Int. Immunopharmacol.* **42**, 18–24 (2017).
40. Zhou, W. et al. Network pharmacology to unveil the mechanism of Moluodan in the treatment of chronic atrophic gastritis. *Phytomedicine* **95**, 153837 (2022).
41. Mochida, K., Koda, S., Inoue, K. & Nishii, R. Statistical and machine learning approaches to predict gene regulatory networks from transcriptome datasets. *Front. Plant. Sci.* **9**, (2018).
42. Nadeem, U. et al. Using advanced bioinformatics tools to identify novel therapeutic candidates for age-related macular degeneration. *Transl Vis. Sci. Technol.* **11**, 10 (2022).
43. Shannon, P. et al. Cytoscape: a software environment for integrated models of biomolecular interaction networks. *Genome Res.* **13**, 2498–2504 (2003).
44. Szklarczyk, D. et al. The STRING database in 2023: protein–protein association networks and functional enrichment analyses for any sequenced genome of interest. *Nucleic Acids Res.* **51**, D638–D646 (2023).
45. Nogales, C. et al. Network pharmacology: curing causal mechanisms instead of treating symptoms. *Trends Pharmacol. Sci.* **43**, 136–150 (2022).
46. Bader, G. D. & Hogue, C. W. An automated method for finding molecular complexes in large protein interaction networks. *BMC Bioinform.* **4**, 2 (2003).
47. Schneider, C. A., Rasband, W. S. & Eliceiri, K. W. NIH Image to ImageJ: 25 years of image analysis. *Nat. Methods* **9**, 671–675 (2012).
48. O'Boyle, N. M. et al. Open Babel: An open chemical toolbox. *J. Cheminform.* **3**, 33 (2011).
49. Burley, S. K. et al. RCSB Protein Data Bank (RCSB.org): delivery of experimentally-determined PDB structures alongside one million computed structure models of proteins from artificial intelligence/machine learning. *Nucleic Acids Res.* **51**, D488–D508 (2023).
50. Varadi, M. et al. AlphaFold protein structure database in 2024: providing structure coverage for over 214 million protein sequences. *Nucleic Acids Res.* **52**, D368–D375 (2024).
51. Valdés-Tresanco, M. S., Valdés-Tresanco, M. E., Valiente, P. A. & Moreno, E. AMDock: a versatile graphical tool for assisting molecular docking with Autodock Vina and Autodock4. *Biol. Direct.* **15**, 12 (2020).


## Acknowledgements

This research was supported by Zhejiang Provincial Natural Science Foundation of China under Grant No. LQ23H270015, Zhejiang Provincial Project of Traditional Chinese Medicine Science and Technology No. 2024ZF115, Zhejiang Chinese Medical University Postgraduate Scientific Research Fund Project (No. 2022YKJ07), National Natural Science Foundation of China No. 82305070, and Zhejiang Province Medical and Health Technology Plan Project No. 2024KY1227.

## Author contributions

K.Z. and S.C. performed the experiments and wrote the paper, L.J. and L.X. performed the experiments, Q.Z. and Y.Z. analyzed the results, Q.D. designed and supervised the study, S.W. wrote the paper, designed and super-

vised the study. All authors reviewed the manuscript.

## Declarations

## Competing interests
The authors declare no competing interests.

## Additional information
**Supplementary Information** The online version contains supplementary material available at https://doi.org/10.1038/s41598-024-77897-3.

**Correspondence** and requests for materials should be addressed to Q.D. or S.W.

**Reprints and permissions information** is available at www.nature.com/reprints.

**Publisher's note** Springer Nature remains neutral with regard to jurisdictional claims in published maps and institutional affiliations.